Oscillations of zonal flows in stellarators

P. Helander, A. Mishchenko, R. Kleiber and P. Xanthopoulos

Max-Planck-Institut für Plasmaphysik, 17491 Greifswald, Germany

The linear response of a collisionless stellarator plasma to an applied radial electric field is calculated, both analytically and numerically. Unlike in a tokamak, the electric field and associated zonal flow develop oscillations before settling down to a stationary state, the so-called Rosenbluth-Hinton flow residual. These oscillations are caused by locally trapped particles with radially drifting bounce orbits. These particles also cause a kind of Landau damping of the oscillations that depends on the magnetic configuration. The relative importance of geodesic acoustic modes and zonal-flow oscillations therefore varies among different stellarators.

1 Introduction

In the present article we explore the collisionless evolution of zonal flows in stellarators. This topic has been the subject of recent interest [1, 2, 3, 4], partly because of the suggestion by Watanabe, Sugama and Ferrando-Margalet [5] that the linear neoclassical damping of zonal flows can be of decisive importance for regulating the nonlinear turbulence level. The experimental and numerical evidence for this is still scant, but in any case the linear neoclassical response of the plasma to an applied electric field is something that needs to be understood and can serve as a non-trivial test on gyrokinetic codes.

In a tokamak, the plasma partly shields out an applied radial electric field, because the ion orbits are polarisable: their radial centre of gravity moves in the direction of the applied field (although the bounce points do not move). The plasma thus acts as a dielectric and the residual electric field is smaller than the applied one. Something similar happens in a stellarator [1, 2, 3], but the presence of locally trapped particles leads to qualitatively new behavior. In Ref. [4] it was predicted that the response of the plasma should, in fact, be oscillatory. This occurs because a stellarator plasma does not act simply as a dielectric. In addition to the polarisation of the orbits, there is an effect having to do with the fact that locally trapped orbits drift radially. If an electric field is applied at $t = 0$, these drifts initially vanish on a flux-surface average, because there are as many inward as outward drifting particles on each flux surface. But as time proceeds and these particles drift radially they either gain or lose energy from the electric field, which affects their drift velocity. A net radial current thus arises which is proportional to the time integral of the applied voltage – just like the current in an inductor. The plasma thus acts like an LC-circuit and produces an oscillatory response.

In the present paper we develop the theory of these zonal-flow oscillations further and show that they undergo a kind of Landau damping. If the electric field has a radial variation, particles with different energies phase-mix because they drift radially with different speeds. The strength of this damping is found to depend on the magnetic configuration. We also confirm the existence of zonal-flow oscillations in gyrokinetic simulations. Two different numerical codes are used for this purpose, one local (flux-tube) and one global. The local code is GENE, a continuum code originally developed

for tokamaks and later modified to account for stellarator geometry. The global code is EUTERPE, which based on the particle-in-cell method and solves the gyrokinetic equation in arbitrary stellarator-symmetric geometry. Landau-damped zonal-flow oscillations are found to exist in both types of simulations, as predicted by the analytical theory, but their persitence is very different in different magnetic configurations. Once the oscillations have been Landau damped, there is still a finite residual electric field, just like in the tokamak, and the magnitude of this also depends on the magnetic configuration. It is the level of this residual field that has been suggested to affect the saturated turbulent state of the plasma [5].

The remainder of the paper is organized as follows. In the next section, the theory of Ref.[4] is extended to include the radial drift acting on the perturbed particle distribution function. This is shown to lead to phase mixing and Landau damping in the following section, which is followed by a section where the late-time behavior is computed. The numerical results are described in the penultimate section, which is followed by the conclusions.

2 Initial-value problem

We consider the so-called Rosenbluth-Hinton problem [6] in a stellarator, i.e., we calculate the collisionless, linear response of the plasma to a radial electric field imposed at $t = 0$, restricting our attention to time scales much longer than the bounce time. The electrostatic potential ϕ is then constant on flux surfaces, and its evolution needs to be calculated consistently with the distribution functions f_a for each species a. These satisfy the drift kinetic equation

$$\frac{\partial f_a}{\partial t} + (v_\parallel \mathbf{b} + \mathbf{v}_d) \cdot \nabla f_a - e_a (\mathbf{v}_d \cdot \nabla \phi) \frac{\partial f_a}{\partial \epsilon} = 0,$$

where the independent variables are the kinetic energy $\epsilon = m_a v^2/2$ and the magnetic moment $\mu = m_a v_\perp^2/2B$. The drift velocity is denoted by $\mathbf{v}_d$ and $\mathbf{b} = \mathbf{B}/B$ is the unit vector along the magnetic field. We linearise the kinetic equation in the smallness of $\Phi_a = e_a\phi/T_a \ll 1$, taking the equilibrium to be Maxwellian, $f_{a0} = n_a(m_a/2\pi T_a)^{3/2} \exp(-x^2)$ with $x^2 = m_a v^2/2T_a$, and obtain in first order

$$\frac{\partial f_{a1}}{\partial t} + (v_\parallel \mathbf{b} + \mathbf{v}_d) \cdot \nabla f_{a1} = -\frac{e_a \phi'}{T_a} (\mathbf{v_d} \cdot \nabla r) f_{a0},$$

where r is an arbitrary flux-surface label and $\phi' = \partial\phi(r,t)/\partial r$. To simplify the analysis, we now take f_{a1} and ϕ to vary as e^{ikr} in the radial direction, with a wavelength $2\pi/k$ that is assumed to be much longer than the gyroradius but smaller than the minor radius. We write

$$f_{a1} = h_a - \Phi_a f_{a0}, \tag{1}$$

and take a Laplace transform,

$$\hat{h}_a = \int_0^\infty h_a e^{-pt} dt,$$

so that

$$p\hat{h}_a + v_\parallel \nabla_\parallel \hat{h}_a + ik\hat{h}_a \mathbf{v}_d \cdot \nabla r = p\hat{\Phi}_a f_{a0} + f_{a1}(0),$$

where the last term represents the intitial condition. It is useful to split the radial drift velocity into an orbit-averaged and a fluctuating part,

$$\mathbf{v}_d \cdot \nabla r = \bar{v}_r + v_\parallel \nabla_\parallel \delta_r,$$

where the orbit-averaged drift velocity $\bar{v}_r$ vanishes for circulating particles. For trapped ones it depends on ϵ, μ, and on the magnetic field in the well where the particle is trapped. The function δ_r depends additionally on the position of the particle and is chosen to be odd in $v_\parallel$. Physically, δ_r represents the radial displacement of the orbit from its mean flux surface. The resulting equation,

$$v_\parallel \nabla_\parallel \hat{h}_a + (p + ik\bar{v}_r + ikv_\parallel \nabla_\parallel \delta_r)\hat{h}_a = p\hat{\Phi}_a f_{a0} + f_{a1}(0), \tag{2}$$

is now easily expanded in $p/\omega_b \ll 1$, so that we consider the evolution on time scales exceeding the inverse bounce frequency ω_b. Expanding $\hat{h}_a = \hat{h}_{a0} + \hat{h}_{a1} + \ldots$ correspondingly gives in zeroth and first order

$$\hat{h}_{a0} = \frac{p\hat{\Phi}_a f_{a0} + f_{a1}(0)}{p + ik\bar{v}_r} \overline{e^{ik\delta_r}} e^{-ik\delta_r}, \tag{3}$$

$$v_\parallel \nabla_\parallel \left(\hat{h}_{a1} e^{ik\delta_r} \right) = (p\Phi_a f_{a0} + f_{a1}(0)) \left(e^{ik\delta_r} - \overline{e^{ik\delta_r}} \right), \tag{4}$$

where the time average over an orbit is denoted by an overbar. The evolution of the electrostatic potential is determined by the radial neoclassical current,

$$\Gamma_a = \left\langle \int f_a (\mathbf{v}_d \cdot \nabla r) d^3 v \right\rangle = \left\langle \int \left(f_{a1} \bar{v}_r - v_\parallel \delta_r \nabla_\parallel f_{a1} \right) d^3 v \right\rangle, \tag{5}$$

which upon substitution of Eqs. (1), (3) and (4) becomes

$$\hat{\Gamma}_a = -\hat{\Phi}'_a \left\langle \int f_{a0} \frac{\bar{v}_r^2 + \left(1 - \overline{e^{ik\delta_r}} e^{-ik\delta_r}\right)(p/k)^2}{p + ik\bar{v}_r} d^3v \right\rangle$$

$$+ \left\langle \int f_{a1}(0) \frac{\bar{v}_r + \left(1 - \overline{e^{ik\delta_r}} e^{-ik\delta_r}\right) p/ik}{p + ik\bar{v}_r} d^3v \right\rangle \tag{6}$$

after Laplace transformation. This result is valid for radial wavelengths $2\pi/k$ that are short enough to satisfy the eikonal approximation we have employed when replacing radial derivatives by ik. In addition the wave length needs to be longer than the gyroradius since we have used the drift kinetic equation, but the extension to gyrokinetics would be straightforward. In the following, we find it however convenient to specialize to $k\delta_r \ll 1$, so that the wavelength exceeds the orbit width δ_r. Then the current reduces to

$$\hat{\Gamma}_a = -\hat{\Phi}'_a \left\langle \int f_{a0} \frac{\bar{v}_r^2 + p^2\delta_r^2}{p + ik\bar{v}_r} d^3v, \right\rangle \tag{7}$$

where we have neglected the contribution from $f_{a1}(0)$, which turns out to be small.

This current is related to the time variation of the guiding-center density $n_a(r)$ by the continuity equation,

$$p\hat{n}_a = -\frac{1}{V'} \frac{\partial}{\partial r} \left(V' \hat{\Gamma}_a\right),$$

where $V(r)$ is the volume of the flux surface labelled by r. The density is related back to the potential by the gyrokinetic quasineutrality condition,

$$\sum_a \left\langle n_a e_a + \nabla \cdot \left(\frac{m_a n_a \nabla_\perp \phi}{B^2} \right) \right\rangle = 0,$$

which closes the system. After Laplace transformation, we obtain

$$\sum_a \left\langle \frac{m_a n_a}{B^2} |\nabla r|^2 (p\hat{\phi}' - \phi'_0) - e_a \hat{\Gamma}_a \right\rangle = 0,$$

where $\phi'_0(r) = \phi'(r, t = 0)$. This equation expresses an ambipolarity condition, where the first term is the classical polarisation current

$$\left\langle \mathbf{J}_p^{cl} \cdot \nabla r \right\rangle = \sum_a \left\langle \frac{m_a n_a}{B^2} \frac{\partial \mathbf{E}}{\partial t} \cdot \nabla r \right\rangle$$

and $e_a \hat{\Gamma}_a$ the corresponding neoclassical current. The latter consists according to Eq. (7) of two parts: a neoclassical polarisation current related to the guiding-centre orbit width δ_r (which also exists in tokamaks) and a current caused by the cross-field

drift $\bar{v}_r$ of locally trapped particles. This drift is specific to stellarators and makes the electrons contribute to the radial current to a similar degree as the ions [1, 2, 3, 4].

Finally, upon substituting Eq. (6) we find

$$(p + L(p))\hat{\phi}' = \phi_0', \tag{8}$$

where

$$L(p) = \sum_a \frac{e_a^2}{\Lambda_0 T_a} \left\langle \int f_{a0} \frac{\bar{v}_r^2 + p^2 \delta_r^2}{p + ik\bar{v}_r} d^3v \right\rangle, \tag{9}$$

and we have defined

$$\Lambda_0 = \left\langle \frac{|\nabla r|^2}{B^2} \right\rangle \sum_a m_a n_a. \tag{10}$$

This result agrees with Ref. [4], except for the appearance of $ik\bar{v}_r$ in the denominator of Eq. (9). This is formally a small correction, which however leads to qualilitatively new behavior as it causes the zonal-flow oscillations to undergo Landau damping.

3 Landau damping

Given an arbirtrary initial condition ϕ_0', the subsequent evolution of the electrostatic potential is given by the inverse Laplace transform

$$\phi(t) = \frac{\phi_0'}{2\pi i} \int_{\sigma - i\infty}^{\sigma + i\infty} \frac{e^{pt} dp}{p + L(p)},$$

where the contour should be chosen so as to pass to the right of all poles of the integrand. As in the usual Landau-damping problem, we can deform this contour to the left in the complex plane whilst still making if pass to the right of all poles, and conclude that for large t the potential will evolve as $\phi \propto \exp(p_0 t)$, where p_0 is the root of $p + L(p) = 0$ with the largest real component. If several roots are included, the potential evolves as a sum of such exponentials. In the present problem, the root with the largest real part is trivial, $p = 0$. That this is a root follows from Eq. (9) and $\langle \bar{v}_r \rangle = 0$, and implies that the potential remains finite as $t \to \infty$. However, there is a second root, which is nontrivial and has a real part that is only slightly negative. To find it, we need to continue the function $L(p)$ analytically into the left half of the complex plane, which can be done as follows.

In the integral (9) defining $L(p)$, the bounce-averaged radial drift velocity is proportional to velocity squared,

$$\bar{v}_r = x^2 D(\mathbf{r}, \lambda),$$

with

$$D = \frac{T_a}{e_a}\overline{\left(\frac{2}{B} - \lambda\right)(\mathbf{b}\times\kappa)\cdot\nabla r},$$

where $\kappa = \mathbf{b}\cdot\nabla\mathbf{b}$ is the magnetic-field curvature, $\lambda = \mu/\epsilon$, $x^2 = m_a v^2/2T_a$, and the bounce average has again been denoted by an overbar. D vanishes in the circulating part of phase space, and in the trapped region it is positive on those parts of the flux-surface where the mean drift is outward and negative elsewhere. We decompose (9) accordingly and write $L(p) = L_+(p) + L_-(p)$, where

$$L_\pm(p) = \sum_a \frac{e_a^2}{\Lambda_0 T_a}\left\langle \int f_{a0}\frac{x^4D^2 + p^2\delta_r^2}{p + ikx^2D}H(\pm kD)d^3v\right\rangle,$$

where H is the Heaviside step function, so that only those parts of the flux surface where the mean drift multiplied by k is outward contribute to $L_+(p)$ and only those where it is negative to $L_-(p)$. Using the velocity-space element

$$d^3v = \frac{\pi B v dv^2 d\lambda}{\sqrt{1-\lambda B}},$$

and writing

$$\delta_r = xE(\mathbf{r},\lambda),$$

we obtain

$$L_\pm(p) = \sum_a \frac{n_a e_a^2}{\pi^{1/2}\Lambda_0 T_a}\left\langle B\int_0^{1/B}\frac{H(\pm kD)d\lambda}{\sqrt{1-\lambda B}}\int_0^\infty \frac{x^2D^2 + p^2E^2}{p+ikx^2D}e^{-x^2}x^3dx^2\right\rangle. \qquad (11)$$

The integrand has a pole at $x^2 = ip/kD$, which is unproblematic along the original integration contour, i.e., for $\mathrm{Re}p > 0$. In the integral for $L_+(p)$, where $D > 0$, this pole has positive imaginary part and the contour of integration in the x^2-integral passes below the pole. In order to analytically continue the function $L_+(p)$ to the entire complex plane we thus need to distort the contour of integration so that it always passes below the pole, which has a negative imaginary part when $\mathrm{Re}\,p < 0$, see Fig. 1. Conversely, the x^2-integral in the expression for $L_-(p)$ should always pass above the pole.

It is now straightforward to evaluate the effect of the drift D when the wavelength $2\pi/k$ is sufficiently long. When $kD \ll p$ and D is neglected altogether, we recover the result of Ref. [4],

$$L_+ + L_- = \frac{1}{\Lambda_0}\left(\Lambda_1 p + \frac{\Lambda_2}{p}\right) \equiv L_0(p),$$

where Λ_0 was defined in Eq. (10) and

$$\Lambda_1 = \sum_a \frac{3n_a e_a^2}{4T_a} \left\langle B \int_0^{1/B} \frac{E^2 d\lambda}{\sqrt{1-\lambda B}} \right\rangle, \tag{12}$$

$$\Lambda_2 = \sum_a \frac{15n_a e_a^2}{8T_a} \left\langle B \int_{1/B_{\max}}^{1/B} \frac{D^2 d\lambda}{\sqrt{1-\lambda B}} \right\rangle.$$

We recall that D vanishes in the untrapped region of phase space, $\lambda < 1/B_{\max}$, where $B_{\max}$ denotes the maximum value of the mangetic field strength on the flux surface in question. The root to $p + L(p) = 0$ is now given by

$$p_0 = \pm i \sqrt{\frac{\Lambda_2}{\Lambda_0 + \Lambda_1}} = i\Omega_0, \tag{13}$$

so that the electric field undergoes harmonic oscillations. If the drift is included, the frequency acquires a small imaginary part,

$$p = i\Omega_0 - \gamma,$$

with $\gamma \ll \Omega_0$, corresponding to a weak Landau damping. Mathematically, this arises from the pole

$$x^2 = ip/kD \simeq -\Omega_0/kD,$$

in the x^2-integral (11). Since this integral is taken only along the positive x^2-axis, such a pole will contribute to $L_-(p)$ if $\Omega_0 > 0$ and to $L_+(p)$ if $\Omega_0 < 0$. In either case, the contribution is equal to

$$L_{\rm res}(i\Omega_0) \simeq \sum_a \frac{\pi^{1/2} n_a e_a^2 |\Omega_0|^{5/2}}{\Lambda_0 T_a k^{7/2}} \left\langle B \int_{1/B_{\max}}^{1/B} H\left(-\frac{\Omega_0}{kD}\right) \frac{e^{-|\Omega_0/kD|} d\lambda}{|D|^{3/2}\sqrt{1-\lambda B}} \right\rangle,$$

where the Heaviside function restricts the surface integral to be taken only over that part of the flux surface where the drift has the correct sign for a resonance to occur. The damping rate is finally obtained from the root to

$$i\Omega_0 - \gamma + L_0(i\Omega_0 - \gamma) + L_{\rm res}(i\Omega_0) = 0,$$

which is approximately

$$\gamma = \frac{L_{\rm res}(i\Omega_0)}{2(1 + \Lambda_1/\Lambda_0)}. \tag{14}$$

The approximations made in this derivation require $\Omega_0/kD \gg 1$ so that the damping rate is small, $\gamma \ll \Omega_0$. Since $D/\Omega_0 \sim E \sim \delta_r$ according to Eq. (13), the calculation is formally consistent if $k\delta_r \ll 1$, as already assumed in the derivation of Eq. (9).

However, the eikonal approximation requires $ka \gg 1$, where a is the plasma radius, and we thus require $k\delta_r \ll 1 \ll ka$. In fact, the relative error introduced by the eikonal approximation can be shown to be of order $1/(k^2 a\delta_r)$, so we actually require

$$1 \ll \frac{1}{k\delta_r} \ll ka.$$

Although this condition can formally be satisfied in the small-gyroradius limit, an actual device may not be large enough to make the approximation accurate. The analytical results should therefore be seen more as a qualitative guide to the physics of zonal flow oscialltions than a quantitative prescription for the calculation of their frequencies and damping rates. If higher accuracy is warranted, it is straightforward to use Eq. (6), which is valid down to $k\delta_r = O(1)$, at the expense of making the integrals more complicated [7].

4 Late-time behavior

From the analysis in the previous section, it is clear that Landau damping occurs of the zonal-flow oscillations found in Ref. [4]. This damping is due to phase mixing that arises because particles with different energies have different radial drift velocities. As in the original Landau problem, the damping is exponentially weak when the wavelength is long, but unlike the original problem, the damping is not complete: the oscillations are not damped all the way to zero.

As already mentioned, this follows from the fact that besides the root to the equation $p+L(p) = 0$ that was found in the previous section there is another, trivial, root, $p = 0$. The final-value theorem for Laplace transforms together with Eq. (8) implies

$$\lim_{t\to\infty} \frac{\phi'(t)}{\phi'_0} = \lim_{p\to 0} \frac{p\hat{\phi}'(p)}{\phi'_0} = \lim_{p\to 0} \frac{p}{p + L(p)} \neq 0, \tag{15}$$

since $L(p) = O(p)$ for small p. Indeed, for small p, we may expand the first term of the x-integral in Eq. (11),

$$\frac{x^2 D^2}{p + ikDx^2} = \frac{D}{ik}\left(1 - \frac{p}{ikDx^2} + \cdots\right),$$

to find (in the trapped region)

$$D^2 \int_0^\infty \frac{x^5 e^{-x^2}}{p + ikx^2 D} dx^2 = \frac{\pi^{1/2} p}{2k^2} + O(p^{5/2}),$$

where we have omitted terms that are odd in D and therefore vanish on a flux-surface average. Hence

$$L(p) = \frac{\Lambda_1 + \Lambda_3}{\Lambda_0} p + O(p^{5/2}), \tag{16}$$

with

$$\Lambda_3(k) = \sum_a \frac{n_a e_a^2}{k^2 T_a} \left\langle \sqrt{1 - \frac{B}{B_{\max}}} \right\rangle, \tag{17}$$

where $\langle \sqrt{1 - B/B_{\max}} \rangle$ is the fraction of trapped particles on the flux surface in question. The final value of the zonal-flow potential (15) thus becomes

$$\lim_{t\to\infty} \frac{\phi'(t)}{\phi_0'} = \frac{\Lambda_0}{\Lambda_0 + \Lambda_1 + \Lambda_3(k)}.$$

We now estimate the size of the various terms in this expression, letting

$$\sqrt{\epsilon} \sim \left\langle \sqrt{1 - \frac{B}{B_{\max}}} \right\rangle$$

denote the fraction of trapped particles and

$$E \sim \frac{v_r}{\omega_b} \sim \frac{q\rho}{\sqrt{\epsilon}},$$

their typical orbit width, with $q = \iota^{-1}$ the safety factor and ρ the gyroradius. The trapped particles provide the dominant contribution to the integral (12) in the definition of Λ_1,

$$\left\langle B \int_0^{1/B} \frac{E^2 d\lambda}{\sqrt{1 - \lambda B}} \right\rangle \sim \frac{q^2 \rho^2}{\sqrt{\epsilon}},$$

and we conclude that

$$\frac{\Lambda_1}{\Lambda_0} \sim \frac{q^2}{\sqrt{\epsilon}},$$

$$\frac{\Lambda_3}{\Lambda_0} \sim \frac{\sqrt{\epsilon}}{k^2 \rho_i^2},$$

so that

$$\lim_{t\to\infty} \frac{\phi'(t)}{\phi_0'} = \left(1 + \frac{\alpha q^2}{\sqrt{\epsilon}} + \frac{\beta\sqrt{\epsilon}}{k^2\rho_i^2} \right)^{-1}, \tag{18}$$

where α and β are constants of order unity (see also Ref. [8]). (In a circular tokamak with large aspect ratio, $\alpha = 1.6$ [6].) The β-term is formally larger than the α-term by a factor $(k\delta_r)^2$, with δ_r taken for trapped ions, so the residual flow level is correspondingly smaller in a stellarator than in a tokamak (if indeed $k\delta_r < 1$). It is important to note that the contribution from the electrons is as important as that from the ions: both

species contribute to the sum in Eq. (17) and thus to the reduction of the residual zonal flow (18).

Before concluding this section, we note that the presence of a term proportional to $p^{5/2}$ in Eq. (16) implies that, in addition to the the poles at $p = 0$ and $p = \pm i\Omega_0 - \gamma$, the response function has a branch cut emanating from the origin. This can be traced back to the fact that the analytical continuation from positive to negative Re p that we carried out in the previous section is, in fact, path-dependent. Referring to Figure 2, when the analytical continuation from a point p_1 in the right half-plane to p_2 in the left half-plane is carried out, it matters whether the path followed passes below or above the origin. This is because the x^2-integral in Eq. (11) is only carried out along the positive real axis and if we, for example, consider $L_+(p)$ so that $D > 0$, the pole $x_0^2 = ip/kD$ will cross the positive x^2-axis only if the lower path in Fig. 2 is followed. In addition to the poles at the origin and at $p = \pm i\Omega_0 - \gamma$, there is thus a branch cut that can be taken to follow the negative real axis. Mathematically, this is reflected in the fact that according to Eq. (16) the reponse function has the structure

$$\frac{\hat{\phi}'(p)}{\phi_0'} = \frac{1}{p + L(p)} = \frac{c_0}{p + c_1 p^{5/2} + \cdots} = c_0 \left(\frac{1}{p} - c_1 p^{1/2} + \cdots \right)$$

at the origin. Adding the contribution from the poles at $p = \pm i\Omega_0 - \gamma$, we conclude that the full late-time behaviour is of the form

$$\frac{\phi'(t)}{\phi_0'} \sim c_0 \left(1 + \frac{c_1}{2\pi^{1/2} t^{3/2}} \right) + c_+ e^{(i\Omega_0 - \gamma)t} + c_- e^{(-i\Omega_0 - \gamma)t}.$$

Thus, the oscillations are damped exponentially whilst the residual level is approached algebraically. A similar algebraic decay has earlier been established for ion-temperature-gradient-driven modes [9, 10].

5 Numerical simulations

In order to verify the analytical predictions, we have carried out numerical simulations using two independent and complementary gyrokinetic codes, GENE and EUTERPE. GENE is an Eulerian code solving the gyrokinetic system of equations in either tokamak [11] or stellarator [12] geometry. It has recently been extended to cover the full minor radius in tokamak geometry, but the stellarator version operates in a flux tube with periodic boundary conditions. EUTERPE is a global particle-in cell-code using full

stellarator geometry [13, 14]. The simulations shown below are linear, collisionless and employ adiabatic electrons, but the codes are also capable of simulations involving multiple kinetic species, electromagnetic effects, collisions, and nonlinear terms. As already noted, in stellarators the contribution from the electrons is as important for the evolution of zonal flows as that from the ions, so the electrons ought to be treated kinetically. They should then increase the zonal-flow oscillation frequency (and affect their damping rate) by contributing to Λ_2, and reduce the residual flow through their contribution to Λ_3, which should have an effect on the turbulence level in nonlinear simulations. In the present simulations, however, our aim is simply to verify the main features of the zonal flows identified above and we neglect the electron contribution to keep the calculations as simple as possible.

Two specific stellarators have been simulated, the Large Helical Device (LHD) and Wendelstein 7-X (W7-X), and the behaviour of zonal flows and geodesic acoustic modes (GAMs) was found to be different in the two devices. Figure 3 shows the evolution of the flux-tube averaged potential, calculated linearly as in Sec. II with the GENE code in the two devices. An initial perturbation of the density and potential was applied to a flux tube intersecting the midplane in an up-down symmetric poloidal section of the plasma. It is important to choose such a stellarator-symmetric flux tube, because it is necessary to ensure that certain averages which appear in the theory above and vanish when they are extended over the entire flux surface (such as $\langle D \rangle = 0$) retain this property when the average is instead taken over a flux tube of finite length. When this is the case, qualitatively similar results are obtained in flux-tube and global simulations. The minor radius of the simulated flux tubes was chosen to be $r = 0.6$ in both devices, where r is defined as the square root of the toroidal magnetic flux normalised to its value at the plasma edge. It is obvious from the figure that the oscillation frequency is much larger in LHD than in W7-X. In LHD the oscillations are predominantly GAMs, whilst in W7-X they are mostly zonal-flow oscillations of the type calculated above. The reason for the different behaviour has to do with the respective damping rates. Geodesic acoustic modes are damped by ordinary (parallel) Landau damping, which results in a damping rate proportional to [1]

$$\gamma_{\mathrm{GAM}} \sim -\exp\left(-cq_*^2\right),$$

where c is a constant and q_* is a quantity that is approximately, but not exactly, equal

to the safety factor (inverse rotational transform). Because of its sensitivity to q_*, the damping of GAMs is much greater in W7-X than in LHD. The safety factor is equal to $1/\iota = 1.9$ on the flux surface under consideration in LHD, which is almost twice as large as in W7-X. Conversely, the damping of zonal-flow oscillations, which is approximately given by Eq. (14), is stronger in LHD than in W7-X. This can be traced back to the fact that W7-X has smaller neoclassical losses than LHD. In the present theory, the unconfined orbits enter through the quantity D, which in turn affects the zonal-flow oscillation frequency Ω_0. In a stellarator that has been well optimized for neoclassical confinement, Ω_0 is small, and vanishes in the limit of perfect omnigeneity (e.g., in a tokamak). The Landau damping (14) then becomes small, which is what makes the zonal-flow oscillations visible in W7-X, while in LHD they are so quickly damped that they are practically indiscernable in Fig. 3. They nevertheless occur in LHD, as is illustrated by Fig. 4, where a similar, but global, simulation has been carried out with the EUTERPE code. In this simulation, a large-scale perturbation has been applied to LHD, by choosing the initial density perturbation to be proportional to $\cos \pi s$, where $s \in [0, 1]$ is the normalised toroidal flux. Superimposed on the GAMs, a low-frequency oscillation is barely visible. Again, the GAMs are much more prominent than these slower oscillations, but the latter are clearly visible in Figs. 5-6, where a Fourier transform has been taken of the LHD signals from Figures 3 and 4, respectively. The zonal flow oscillations show up in these figures as a peak in the spectrum at a frequency roughly an order of magnitude below that of the GAMs. In addition, there is third peak at zero frequency, corresponding to the residual zonal flow calculated in the previous section. As predicted by Eq. (18), this level depends on the radial wavenumber, and the corresponding numerical result for the global LHD simulation is shown in Fig. 7. That the oscillations indeed correspond to GAMs and zonal-flow oscillations, respectively, is confirmed by analysis of the poloidal side bands (not shown), which are qualitatively different for these oscillations.

6 Conclusions

As first predicted in Ref. [4], the response of a stellarator plasma to an applied radial electric field is oscillatory, even on time scales exceeding the bounce frequency so

that GAMs have been damped away. We have confirmed this prediction by gyrokinetic simulations, both in local (flux-tube) and global geometry, using two independent gyrokinetic codes. These simulations also include GAMs, and it is observed that the relative importance of GAMs and zonal-flow oscillations is sensitive to the magnetic geometry, which affects the oscillation frequencies and damping rates. This can be understood from an extension of the theory undertaken in the present paper to include the effect of magnetic drifts on the perturbed distribution function. Because particles of different energy have different radial drift velocities, they undergo phase mixing in a radially varying electric field. The damping of GAMs depends exponentially on the rotational transform squared and becomes very strong in a tightly wound field, whilst the damping of zonal-flow oscillations (as well as their frequency) is related to the degree of neoclassical orbit optimization. In our simulations, GAMs were weakly damped and zonal-flow oscillations stongly damped in one case (LHD) and vice versa in another (W7-X). Once these respective oscillations have died out, a finite "Rosenbluth-Hinton" residual flow remains, whose level also depends on the magnetic configuration. It has been suggested that this residual can be instrumental in regulating the turbulent transport level, but it appears equally possible that it could be the *approach* to this state (for instance the oscillations) that matters, if the linear properties of zonal flows are at all important. This issue will be expored in a future publication.

Acknowledgement

We are very grateful to an anonymous referee for pointing out the path-dependence of the analytical continuation and the resulting algebraic approach to the residual zonal-flow level.

References

[1] H. Sugama and T.-H. Watanabe, Phys. Plasmas **13**, 012501 (2006); **14**, 079902 (2007).

[2] H. Sugama and T.-H. Watanabe, Phys. Plasmas **16**, 056101 (2009).

[3] H.E. Mynick and A.H. Boozer, Phys. Plasmas **14**, 072507(2007).

[4] A. Mishchenko, P. Helander, and A. Könies, Phys. Plasmas **15**, 072309 (2008).

[5] T.-H. Watanabe, H. Sugama, and S. Ferrando-Margalet, Phys. Rev. Lett. **100**, 195002 (2008).

[6] F.L. Hinton and M.N. Rosenbluth, Plasma Phys. Contr. Fusion **41**, A653 (1999).

[7] Y. Xiao, P. J. Catto, and W. Dorland, Phys. Plasmas **14**, 055910 (2007).

[8] H. Sugama and T.-H. Watanabe, Contrib. Plasma Phys **50**, 571 (2010).

[9] , T. Kuroda, H. Sugama, R. Kanno, M. Okamoto and W. Horton, J. Phys. Soc. Japan **67**, 3787 (1998).

[10] H. Sugama, Phys. Plasmas **6**, 3527 (1999).

[11] F. Jenko, W. Dorland, M. Kotschenreuther and B.N. Rogers, Phys. Plasmas **7**, 1904 (2000).

[12] P. Xanthopoulos, W.A. Cooper, F. Jenko, Yu. Turkin, A. Runov and J. Geiger, Phys. Plasmas **16**, 082303 (2009).

[13] V. Kornilov, R. Kleiber, R. Hatzky, L. Villard, and G. Jost, Phys. Plasmas **11**, 3196 (2004).

[14] R.Kleiber, in *Theory of Fusion Plasmas*, p.136, AIP Conference Proceedings 871 (2006).

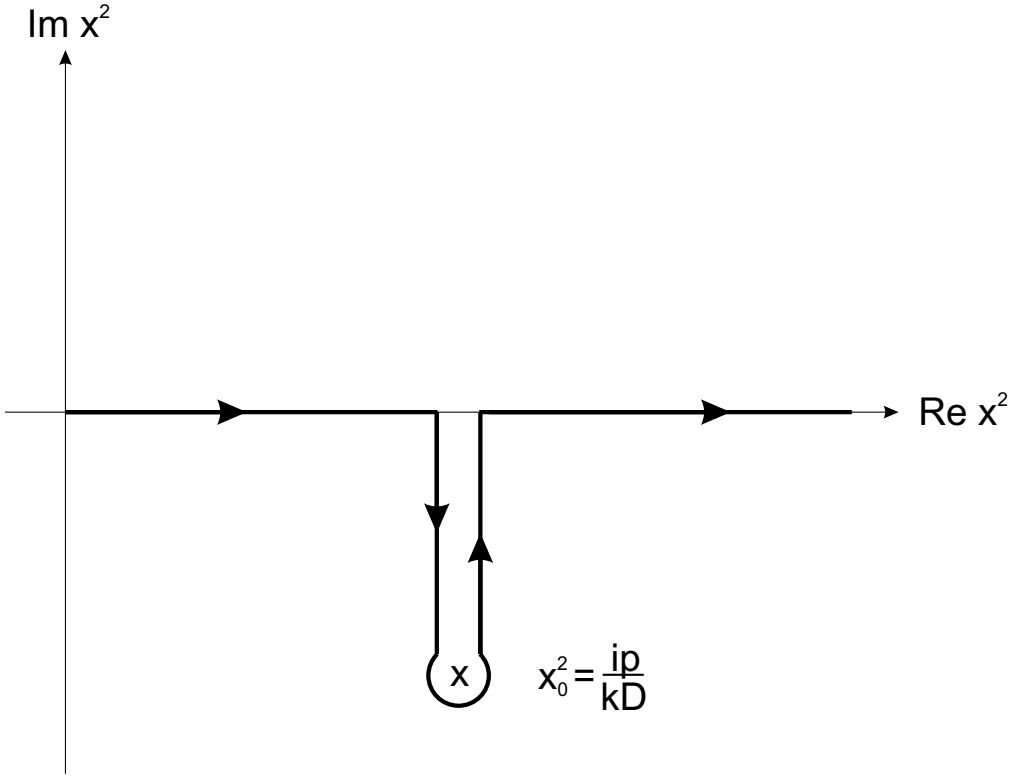

Figure 1: *Integration path for $L_+(p)$ in Eq. (11).*

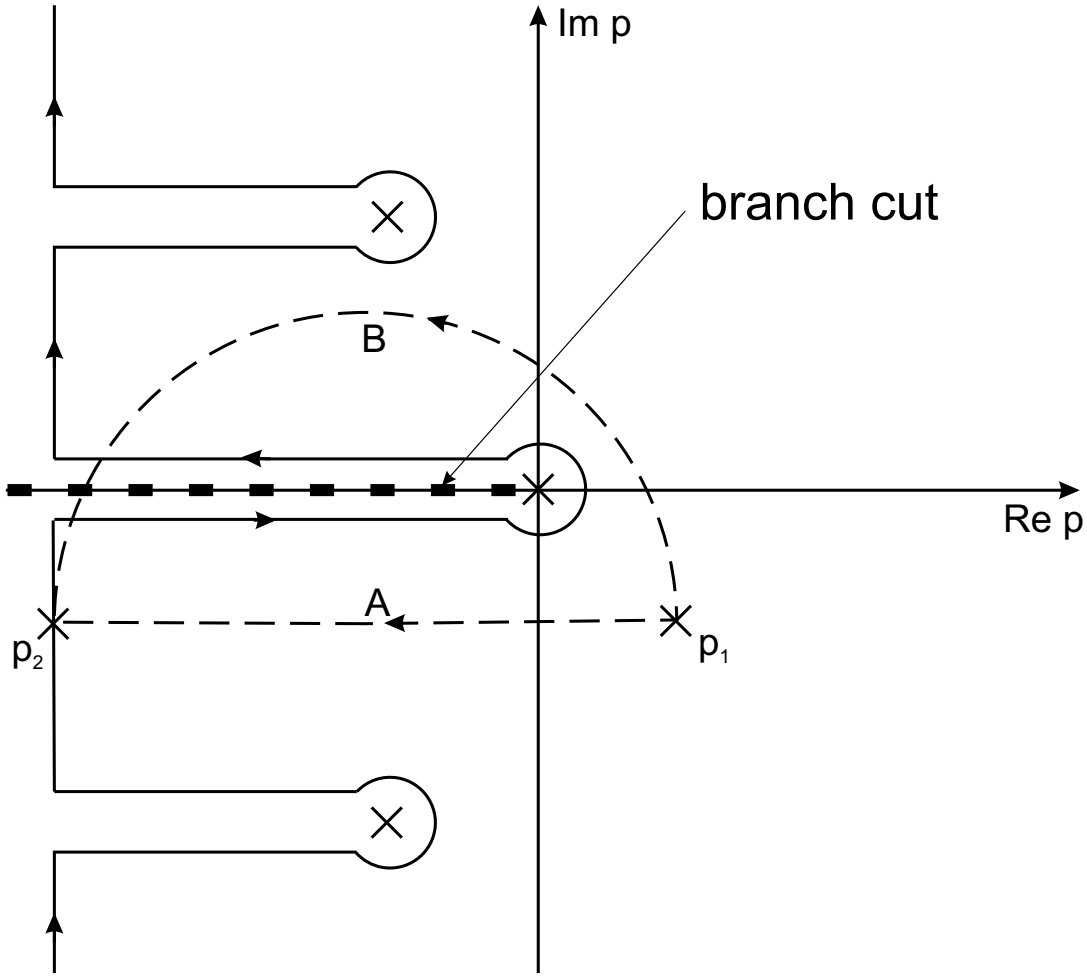

Figure 2: *The integration countour for the inversion of the Laplace transform is shifted to the left, but stays to the right of the poles and the branch cut along the negative real axis. This branch cut arises because of the path-dependence of the analytical continuation, which is different along the paths A and B.*

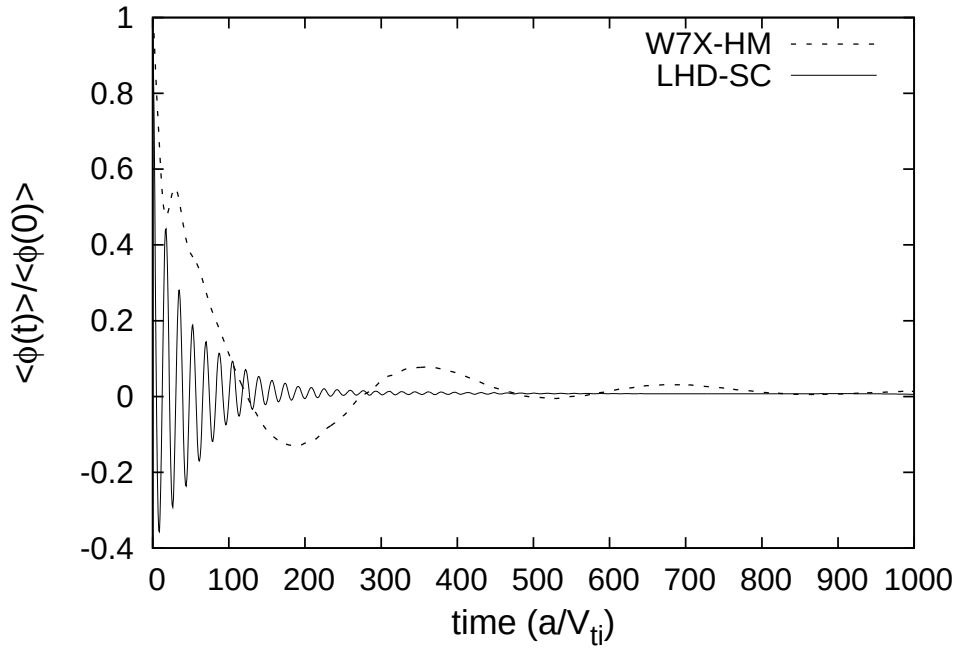

Figure 3: *Zonal-flow response in the standard configuration of LHD and the high-mirror configruation of W7-X. The radial electric field as a function of time after a perturbation* $\cos kr$ *with* $k\rho_{ti} = 0.06$ *has been applied at* $t = 0$.

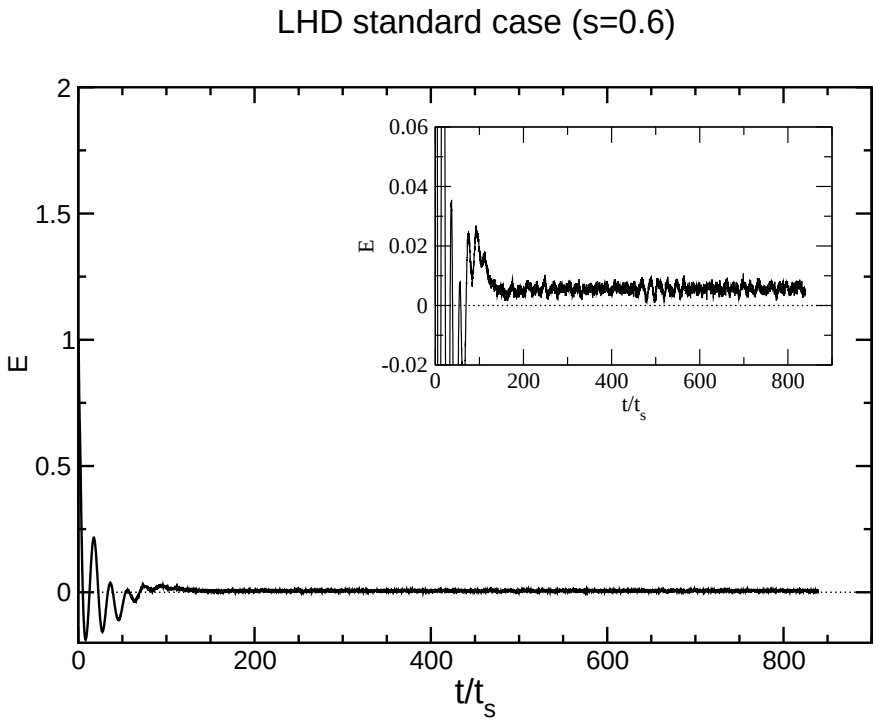

Figure 4: *Zonal-flow response in LHD. The radial electric field as a function of time after a perturbation* $\cos \pi s$ *has been applied at* $t = 0$.

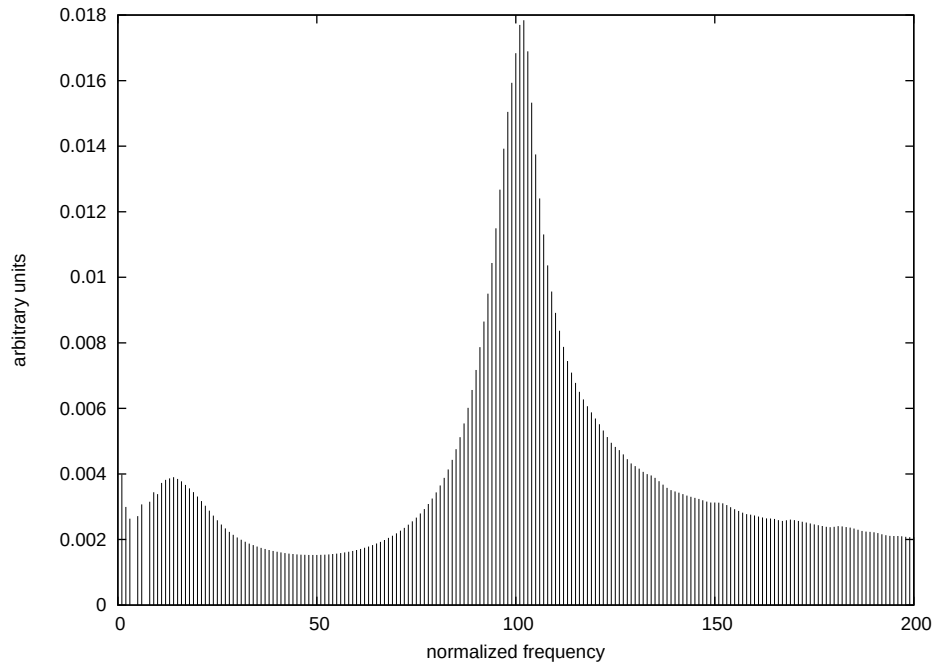

Figure 5: *Fourier transform of the signal from LHD displayed in Fig. 3. Three peaks are visible, corrsponding to the Rosenbluth-Hinton residual at zero frequency, low-frequency oscillations of the zonal flow, and GAMs at high frequency.*

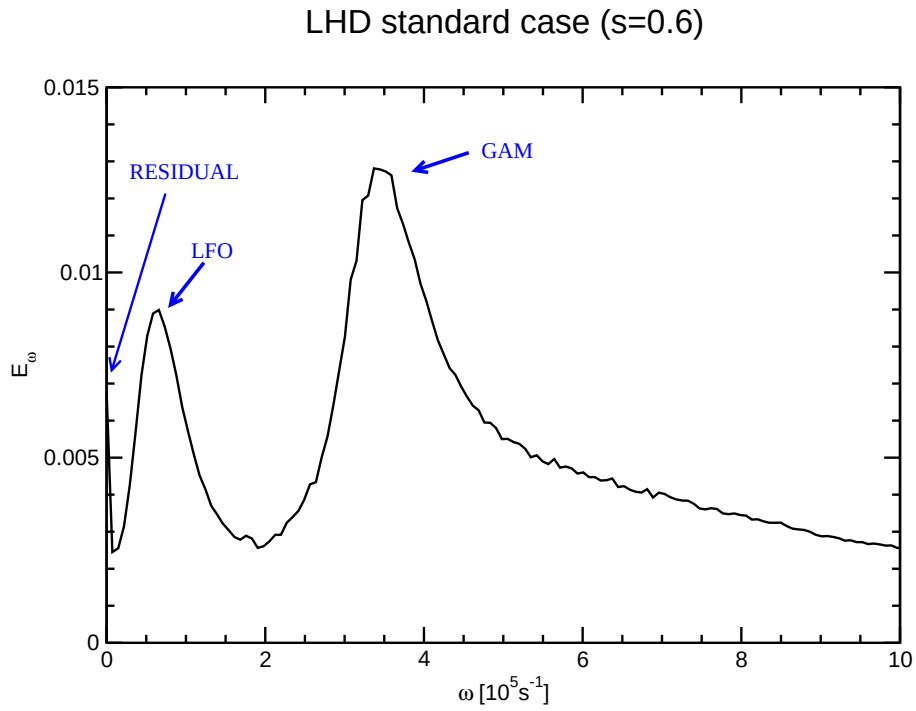

Figure 6: *Fourier transform of the signal displayed in Fig. 4, exhibiting similar peaks as in Fig. 5.*

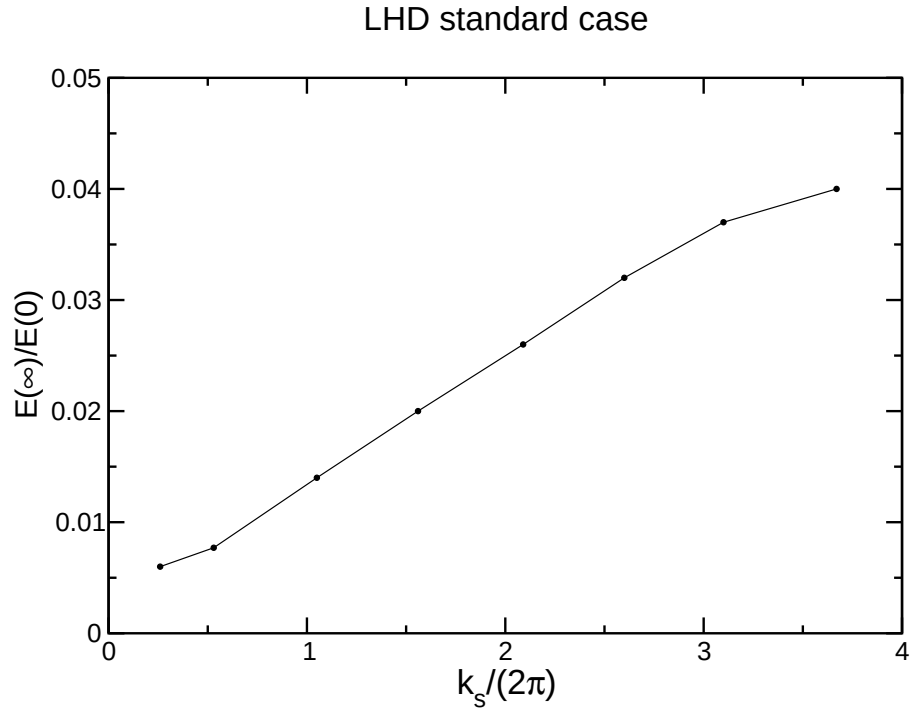

Figure 7: *Final value of the radial electric field, i.e., the Rosenbluth-Hinton residual, as function of radial wave number in LHD.*